

Thermopower and quantum criticality in a strongly interacting system: parallels with the cuprates

Arti Garg^{1,3}, B Sriram Shastry¹, Kieran B Dave²
and Philip Phillips²

¹ Physics Department, University of California, Santa Cruz, CA 95064, USA

² Physics Department, University of Illinois, Urbana Champaign, IL 61801, USA

E-mail: agarg3@ucsc.edu

New Journal of Physics **13** (2011) 083032 (9pp)

Received 14 April 2011

Published 24 August 2011

Online at <http://www.njp.org/>

doi:10.1088/1367-2630/13/8/083032

Abstract. In high T_c superconductors a wide ranging connection between the doping dependence of the transition temperature T_c and the room temperature thermopower Q has been observed. A ‘universal correlation’ between these two quantities exists with the thermopower vanishing at optimum doping as noted by OCTHH (Obertelli, Cooper, Tallon, Honma and Hor). In this work we provide an interpretation of this OCTHH universality in terms of a possible underlying quantum critical point (QCP) at T_c . Central to our viewpoint is the recently noted Kelvin formula relating the thermopower to the density derivative of the entropy. Perspective on this formula is gained through a model calculation of the various Kubo formulas in an exactly solved 1-dimensional model with various limiting procedures of wave vector and frequency.

³ Author to whom any correspondence should be addressed.

Contents

| | |
|---|----------|
| 1. Introduction | 2 |
| 2. Model | 4 |
| 2.1. Choice of current operators | 5 |
| 2.2. Formulae for the thermopower | 6 |
| 3. Conclusions | 8 |
| Acknowledgments | 9 |
| References | 9 |

1. Introduction

Universal properties of strongly correlated matter are particularly interesting, since they hold the promise of revealing the fundamental physics of these systems. An example in the case of heavy fermion systems is the well-known Kadowaki–Woods relation [1] $A\gamma^{-2} \simeq 1.0 \times 10^{-5} \text{ c}$ between the specific heat coefficient γ and A , the T^2 coefficient of the resistivity. Understanding the origin of this universal value has led to considerable theoretical progress [2]. In the case of High T_c materials, Obertelli, Cooper and Tallon (OCT) [3] observed that the thermopower for several cuprates vanishes in the vicinity of optimal doping. Honma and Hor (HH) [4] extended their analysis, which was based on the phenomenological scale $1 - \frac{T_c}{T_c^{\text{max}}} = 82.6(x - 0.16)^2$ [5], by first showing that the thermopower for all the cuprates collapses onto a universal curve as a function of the doping level with a zero crossing at a hole content of $x \approx 0.23$. Since this universal scale is valid for all the cuprates, they then advocated [4] that it can be used as an independent calibration of the doping level. Consequently, they mapped out the phase diagram of the cuprates in which x was determined from the thermopower and not from the Presland [5] scale. Using this scale, they showed [4] that optimal doping for 19 of the 23 cuprates studied corresponded with the zero crossing of the thermopower. The exceptions are 4 single-layer materials. Assuming this is not a coincidence, it is reasonable to conclude that the mechanism of high- T_c and the vanishing of the thermopower [6]⁴ share a common origin.

The observation of OCTHH has stimulated considerable thought in the community [7–10]. In the context of the Hubbard model, some [8, 9] have argued that dynamical spectral weight transfer ceases at the doping at which the thermopower vanishes, thereby defining a quantum phase transition (QPT) where the upper-Hubbard band decouples and Fermi-liquid theory obtains. While cluster calculations on the Hubbard model [11] support this interpretation, no simple model has been studied in which exact statements can be made regarding the vanishing of the thermopower and the onset of a quantum phase transition. The present work is stimulated by this situation, and we present below two key ideas and a set of model calculations that provide a natural framework for understanding such a universality.

The first key idea in our work is the interpretation of the thermopower as being largely determined by *thermodynamics*, rather than transport aspects, such as velocities and relaxation

⁴ There is also discussion of universal behaviour of the thermopower for heavy fermion systems of a rather different character from the one discussed by OCT. The relevant experiments are in [6] and theoretical discussion is in Zlatić *et al* [6].

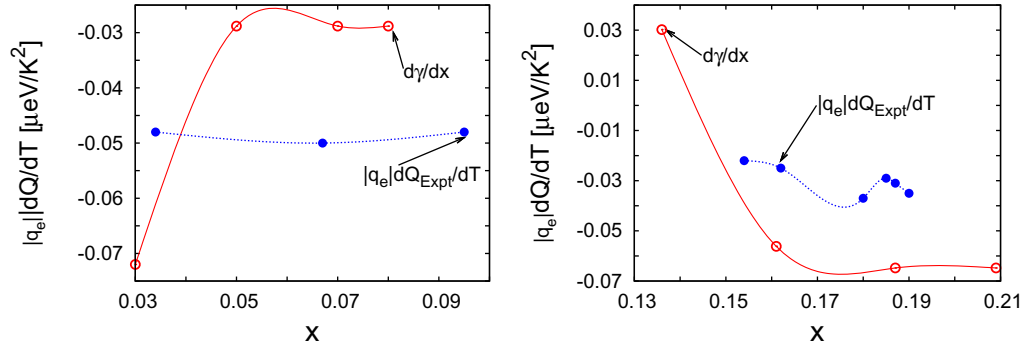


Figure 1. A test of the reliability of the Kelvin formula, as explained in the text, for $\text{Ti}_2\text{Ba}_2\text{CuO}_{6+\delta}$ at $T = 100$ (left) and BSSCO at $T = 120$ (right). The red solid curves are $d\gamma/dx$ and the blue dotted curves are $|q_e|dQ/dT$. These curves would coincide in the $T \rightarrow 0$ limit if the Kelvin formula were exact.

times⁵. While this idea of thermodynamic domination of thermopower cannot be an exact statement, it leads to the Kelvin formula proposed by Shastry and co-workers [10, 14] in the spirit of Lord Kelvin's original treatment [13]. The Kelvin formula for thermopower Q_K is obtained by computing the slow limit of an exact formula at finite q , ω , and is given by⁶

$$Q_K = \frac{1}{q_e} \left(\frac{\partial S}{\partial x} \right)_{T,V}, \quad (1)$$

where S is the entropy density, x is the density of carriers in the system and q_e is the charge of the carriers ($-|q_e|$ for electrons)⁷. In brief, this approximate formula for thermopower captures the enhancements due to all fluctuations that influence the thermodynamics of a many body system. While theoretical benchmarks of this approximation exist [10], it is also useful to check its consequences directly for the high- T_c systems. Using standard thermodynamics, one gets the following relation between the temperature dependence of the Kelvin thermopower and the specific heat variation with particle density x :

$$q_e \frac{\partial Q_K}{\partial T} = \frac{1}{T} \left(\frac{\partial C_v}{\partial x} \right)_{V,T} \xrightarrow{T \rightarrow 0} \left(\frac{\partial \gamma}{\partial x} \right)_{V,T}, \quad (2)$$

where γ is the low-temperature coefficient of the specific heat. This equality comprises a relationship between two independent experiments and can therefore be tested with experimental data. Figure 1 plots the left and right sides of (2) based on thermopower [3]

⁵ This separation of the thermopower into the two components of thermodynamics and transport is well illustrated by rewriting the Mott formula for the thermopower of a weakly diffusive metallic system given in textbooks [12] as

$$Q_{\text{Mott}} = T \frac{\pi^2 k_B^2}{3q_e} \left\{ \frac{d}{d\mu} \ln[\rho(\mu)] + \frac{d}{d\mu} \ln[(\langle v_p^x \rangle)^2 \tau(p, \mu)] \right\},$$

where μ is the chemical potential. In this expression, the first term gives the density of states (and hence thermodynamic) contribution, and the second term gives the transport contribution from the Fermi-surface average of the squared velocity and the relaxation time.

⁶ Throughout this paper, the slow limit denotes taking $\omega \rightarrow 0$ followed by $q \rightarrow 0$, whereas the fast limit denotes $q \rightarrow 0$ followed by $\omega \rightarrow 0$. See [21].

⁷ For applying this formula to holes, we regard x as the hole density and remember to use $q_e = -|q_e|$.

and electronic specific heat data [15, 16] for $\text{Bi}_2\text{Sr}_2\text{CaCu}_2\text{O}_{8+\delta}$ and $\text{Tl}_2\text{Ba}_2\text{CuO}_{6+\delta}$. While the agreement is far from perfect and deviations are certainly expected since the correspondence between the left and right-hand sides of equation (2) is only expected to hold at $T = 0$, the signs and orders of magnitude of each side of (2) are compliant with the data, suggesting the level of accuracy one can expect from the Kelvin formula in these systems.

The second key idea involves an underlying quantum critical point [9, 11] (QCP) as the origin of the OCTHH universality. We suggest that optimum doping corresponds to a QCP at $T = 0$, so that at room temperature, the entropy has a maximum as a function of the density. From the Kelvin formula, this feature would explain why the room temperature thermopower changes sign at optimal doping.

These ideas may be illustrated within a simple fermionic model exhibiting a QCP. The reader is forewarned that this model is quite unphysical because the number of particles is not conserved; nevertheless, its exact solvability makes it invaluable for the purpose at hand. It also has the essential feature that the parameter tuned to reach the QCP is thermodynamically conjugate to the average particle number density. Because the fingerprints of the $T = 0$ transition at finite temperature include a maximum in the entropy as a function of the density, the properties of the model lead naturally to the OCTHH universality.

2. Model

We analyse the anisotropic quantum XY model in the presence of a transverse field in one dimension, which, after a Jordan–Wigner transformation, is described by the fermionic Hamiltonian [17]⁸,

$$\frac{H}{J} = - \sum_i \left[c_i^\dagger c_{i+1} + \Gamma c_i^\dagger c_{i+1}^\dagger + \text{h.c.} \right] - h \sum_i (1 - 2c_i^\dagger c_i). \quad (3)$$

Here $-2h$ is the dimensionless chemical potential. Due to the Γ terms, the number of fermions is not conserved and hence only the average particle number may be fixed. The Hamiltonian can be diagonalized via the Bogoliubov transformation: its eigenvalues are

$$\epsilon_k = \pm 2\sqrt{(h - \cos k)^2 + \Gamma^2 \sin^2 k}, \quad -\pi < k \leq \pi. \quad (4)$$

For any value of Γ , the system has a QCP at $h = 1$, where the spectral gap $\Delta = 2|(1 - h)|$ vanishes continuously. The T - h phase diagram is shown in figure 2(a). There are two low- T phases. For $h < 1$, the low- T phase has an energy gap with a high density of fermions. At $T = 0$, $\Gamma > 0$ and with $|h| \leq 1$, the equal-time spin correlation function $C(R, t = 0) = \langle \sigma_i^x \sigma_{i+R}^x \rangle$ ⁹ in the limit $R \rightarrow \infty$ is nonzero, being equal to [18] $C(\infty, 0) = \frac{1}{2(1+\Gamma)} [\Gamma^2(1 - h^2)]^{\frac{1}{4}}$. This result indicates the presence of magnetic long-range order in the ground state. For $h > 1$, the low- T phase has a spectral gap and with a low number density. It corresponds to a quantum paramagnet in the original spin model.

The lines $\Delta = t$ shown in figure 2(a) have vanishing excitation energies and represent the crossover between the low- T gapped phases and the intermediate phase, where the dimensionless temperature is defined as $t = k_B T/J$. The average particle density

⁸ In Katsura's [17] expressions, we use the notation $J = \frac{1}{2}(J_x + J_y)$ and $\Gamma = \frac{1}{2J}(J_x - J_y)$, where Γ is a dimensionless anisotropy parameter.

⁹ As per the Jordan–Wigner transformation, $\sigma_i^x \sigma_{i+R}^x = (c_i + c_i^\dagger) \prod_{i \leq j < i+R} (1 - 2n_j) (c_{i+R} + c_{i+R}^\dagger)$.

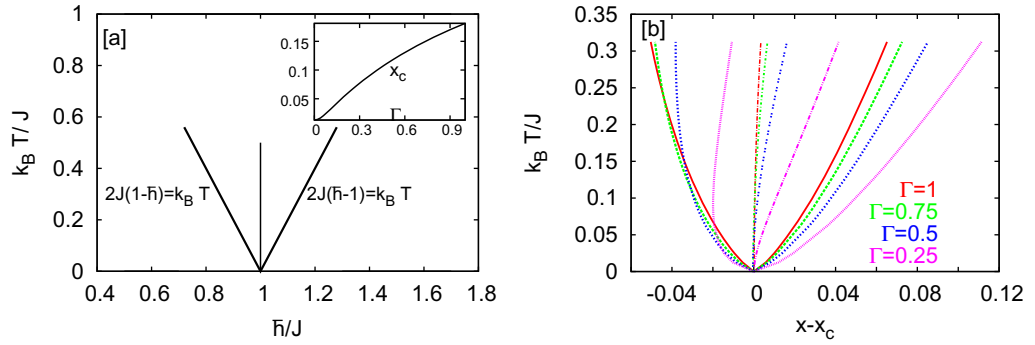


Figure 2. (a) Phase diagram of the 1D quantum model described by the Hamiltonian (3) as a function of $h = \bar{h}/J$ and the temperature $t = k_B T/J$. There is a quantum phase transition at $t = 0$ and $h = 1$ for any value of anisotropy parameter Γ . The entropy is a maximum along the central vertical line that we call the ‘peak line’. The two lines $\Delta = t$ mark the crossovers from the low- T gapped phases to a high- T phase. Inset: the particle density at the critical point $x_c = x(h = 1, T = 0)$, which varies significantly as a function of the anisotropy Γ . (b) $t-(x - x_c)$ phase diagram of the same model for various values of the anisotropy parameter Γ . The peak line and the crossover lines in $t-h$ plane split into many lines in the $t-x$ plane, depending on the value of Γ .

$x = \langle c_i^\dagger c_i \rangle$ is

$$x = \frac{1}{2} \left[1 - \frac{2}{\pi} \int_0^\pi dk \tanh \left(\frac{|\epsilon(k)|}{2t} \right) \frac{(h - \cos k)}{|\epsilon(k)|} \right]. \quad (5)$$

Since at a fixed Γ and temperature, every value of h corresponds to a unique value of the average particle density x , rather than looking at the phase diagram in $t-h$ plane (as shown in figure 2(a)), one can also look at the phase diagram in $t-x$ plane (as shown in figure 2(b)). The value of x at $h = 1$ and $t = 0$ for a given Γ is called the critical particle density x_c for that Γ and is shown in the inset of figure 2(a). Rather than tuning h , one can tune x directly and then a quantum phase transition will take place at $x = x_c$. Due to the nontrivial mapping between h and x in (5), the $t-x$ phase diagram is dependent on the magnitude of Γ , as is shown in figure 2(b). On the other hand, the $t-h$ phase diagram is independent of Γ . The lines corresponding to a vanishing gap at $h = 1$ bend as one moves along the t -axis. The bending angle varies with Γ and is larger for smaller values of Γ . In addition, the crossovers $\Delta = t$ between the low- T and high- T phases move as Γ is varied.

The entropy S for this model may also be found exactly [17]. For all t , S is a maximum as a function of density at $x(h = 1)$, as shown in figure 3. The location of the maximum has its origins in the large number of micro-states possible for the original spin system at $h = 1$. The locus of the maxima of S depends upon Γ and is depicted as the central line in figure 2(b). We term this the ‘peak line’. The peak line has not received attention in earlier works but plays an important role for our purpose.

2.1. Choice of current operators

Equation (3) is the spin-less version of the 1D BCS reduced Hamiltonian. As the total number of particles is not conserved, the standard continuity equation for the charge density $\rho(i)$ does

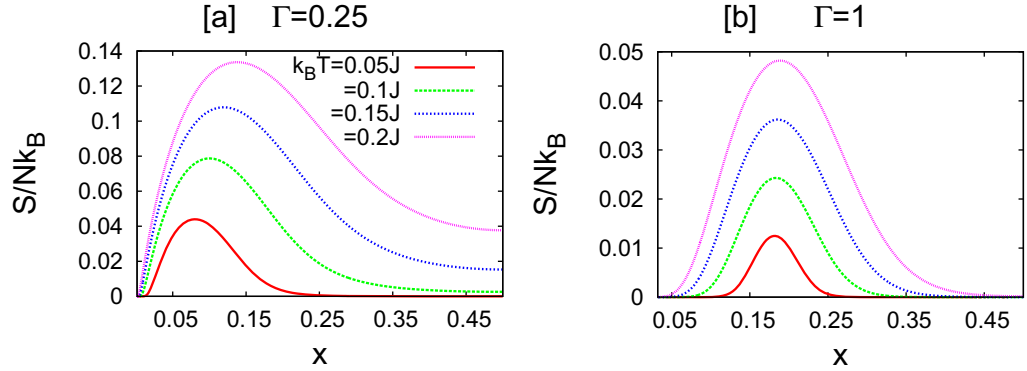


Figure 3. Plots of the entropy S as a function of hole density x at several values of t for (a) $\Gamma = 0.25$ and (b) $\Gamma = 1$. Notice the clear shift in the location of the maximum of S as t increases for $\Gamma = 0.25$. This corresponds to the ‘peak line’ shown in figure 2(b).

not hold and there is some ambiguity as to the choice of local charge current operator. We work with the standard charge current operator given by $J(n) = i(c_n^\dagger c_{n+1} - c_{n+1}^\dagger c_n)$ (here $q_e = 1$). With this choice, the continuity equation for the charge density has pair sources and sinks as in the BCS problem [19]. The continuity equation for the local energy density is standard $\frac{\partial H(n)}{\partial t} + (J_E(n+1) - J_E(n)) = 0$ with energy current operator given by

$$J_E(n) = i(1 - \Gamma^2)(c_{n-1}^\dagger c_{n+1} - c_{n+1}^\dagger c_{n-1}) + i2h(c_n^\dagger c_{n-1} - c_{n-1}^\dagger c_n) + i2h\Gamma(c_{n-1}^\dagger c_n^\dagger - c_n c_{n-1}).$$

It is interesting that both the charge and the energy currents are conserved in this integrable model. However, the calculations do not simplify on account of this feature and so we will not pursue its consequences further.

2.2. Formulae for the thermopower

For a generic 1D system there are four possible linear response formulae for the momentum- and frequency-dependent thermopower:

$$TQ_1(q, \omega) = \frac{\chi_{\rho(q), H^\dagger(q)}(\omega)}{\chi_{\rho(q), \rho^\dagger(q)}(\omega)}, \quad (6a)$$

$$TQ_2(q, \omega) = \frac{\chi_{J(q), H^\dagger(q)}(\omega)}{\chi_{J(q), \rho^\dagger(q)}(\omega)}, \quad (6b)$$

$$TQ_3(q, \omega) = \frac{\chi_{\rho(q), J_E^\dagger(q)}(\omega)}{\chi_{\rho(q), J^\dagger(q)}(\omega)}, \quad (6c)$$

$$TQ_4(q, \omega) = \frac{\chi_{J(q), J_E^\dagger(q)}(\omega)}{\chi_{J(q), J^\dagger(q)}(\omega)}. \quad (6d)$$

Here $A(q) = \sum_n e^{-iq \cdot n} A(n)$ denotes the Fourier transform of the local operator $A(n)$. It can be shown by integration by parts that these four formulas are equivalent only if $[\rho(0), H(0)] = 0$, i.e. particle number is conserved. In the present model since the particle number is not conserved, we evaluate all the expressions individually. The fast limit of (6b) yields the celebrated Kubo formula; the slow limit of (6a) is (1) the Kelvin formula [14].

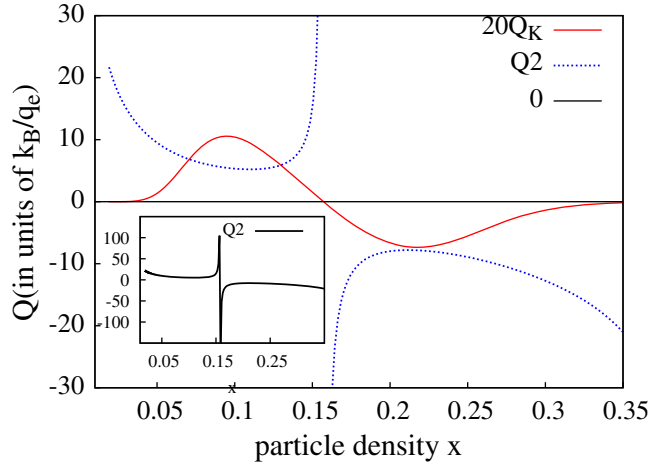


Figure 4. The thermopower, as calculated from the Kubo formula (blue dotted curve) and the Kelvin formula (red solid curve). In both the cases, the thermopower is positive for $x < x_c$ and negative for $x > x_c$. The result shown is for $t = 0.1$ and $\Gamma = 0.75$.

The thermopower was calculated in the slow and fast limits for all four linear response expressions. The Kubo formula is given by

$$Q_{\text{Kubo}} = Q_2^{\text{fast}} = \frac{1}{T} \frac{\sum_k \sin(k) \frac{\partial n_k}{\partial k} F(k, h)}{\sum_k \sin(k) A_1(k) \frac{\partial n_k}{\partial k}}, \quad (7)$$

where $F(k, h) = 2[(h - \cos k)A_1(k) + \Gamma \sin(k)B_1(k)]$, $A_1(k) = \frac{2(h - \cos(k))}{\epsilon(k)}$, $B_1(k) = \frac{2\Gamma \sin(k)}{\epsilon(k)}$, and n_k is the Fermi function. Figure 4 plots the thermopower calculated from the Kubo and the Kelvin formula for $t = 0.1$ and $\Gamma = 0.75$. Note that the Kubo formula result changes sign across the QCP through a divergence. It is positive for $x < x_c$ and negative for $x > x_c$. The Kelvin formula captures the broad features of the thermopower from the Kubo formula result, but it instead changes sign through a zero.

The fast limit of Q_1 and the slow limit of Q_2 are $O(q)$ and hence vanish. Aside from those deriving from Q_1 and Q_2 , there are four more possible expressions for the thermopower which come from the slow and the fast limit of Q_3 and Q_4 :

$$\begin{aligned} TQ_3^{\text{slow}} &= \frac{\sum_k V_H(k) \left(\frac{2 \sin k}{\epsilon(k)} + \frac{2(h - \cos k)\epsilon'(k)}{\epsilon^2(k)} \right) \frac{1 - 2n(k)}{2\epsilon(k)}}{\sum_k V(k) \left(\frac{2 \sin k}{\epsilon(k)} + \frac{2(h - \cos k)\epsilon'(k)}{\epsilon^2(k)} \right) \frac{1 - 2n(k)}{2\epsilon(k)}}, \\ TQ_3^{\text{fast}} &= \frac{\sum_k V_H(k) A_1(k) \frac{\partial n_k}{\partial k}}{\sum_k V(k) A_1(k) \frac{\partial n_k}{\partial k}}, \\ TQ_4^{\text{slow}} &= \frac{\sum_k V_H(k) V(k) \frac{\partial n_k}{\partial \epsilon(k)}}{\sum_k V^2(k) \frac{\partial n_k}{\partial \epsilon(k)}}, \\ TQ_4^{\text{fast}} &= \frac{\sum_k V_H(k) V(k) (\epsilon'(k))^2 \frac{\partial n_k}{\partial \epsilon(k)}}{\sum_k V^2(k) (\epsilon'(k))^2 \frac{\partial n_k}{\partial \epsilon(k)}}. \end{aligned} \quad (8)$$

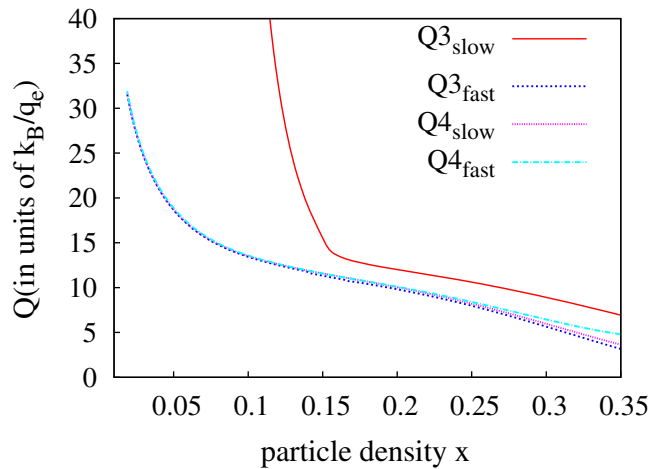


Figure 5. The thermopower, as calculated from the formulae (8). Both the slow and the fast limits of $Q_{3,4}$, which give the thermopower in the presence of a transverse electromagnetic field, are positive for all values of the particle density x and show no sign change across the QCP. The plot shown is for $t = 0.1$ and $\Gamma = 0.75$.

Here $V(k) = 2 \sin(k)$, $V_H(k) = 2hV(k) - 2(1 - \Gamma^2)\sin(2k)$ and $\epsilon'(k) = \frac{\partial \epsilon(k)}{\partial k}$. Figure 5 shows plots of the formulae (8). These four expressions for the thermopower give very similar results: they are positive for all values of the particle density x and do not show any sign change across the QCP.

In the end, one must make a decision as to which thermopower formula is definitive. On the basis of linear response theory, one knows that formulae derived from (6a) and (6b) concern the response of the system to a longitudinal electromagnetic field while formulas (6c) and (6d) concern a transverse electromagnetic field. Since the thermopower measured experimentally is actually the response to a longitudinal electromagnetic field, we believe that only results from (6a) and (6b) contain information about the physical thermopower¹⁰.

3. Conclusions

Supposing that the choice of thermopower formula is correct, the OCTHH universality is partially vindicated by the model. The Kelvin and Kubo formulae for the thermopower exhibit a sign change at $x_c(T) \approx x_c(T = 0)$, in parallel to the case in the cuprate superconductors. Inherently, the model studied here is much too simple to be taken seriously as a microscopic model of a real material: in particular, it can do nothing to correlate optimal doping with a QCP. It does, however, illustrate how a sign change in the thermopower might ultimately be connected to a QCP. It also illustrates how an equilibrium construction such as the Kelvin formula may be used to approximate the behaviour of a transport quantity such as the Kubo formula. Finally,

¹⁰ At this stage it might be useful to notice the difference between this model and the BCS problem. In the BCS problem, one gets accurate response to the transverse electromagnetic field even in simple pairing approximation. However to get the correct response to the longitudinal electromagnetic field, one needs to go beyond the mean field pairing picture and keep collective density fluctuation mode. But in this model there is no analogous possibility like this. Thus we will work with formulas (6a) and (6b) which provide response to a more physical situation.

we point out that the method used by Vidyadhiraja *et al* [11] to locate the quantum critical point relies on the maximum in the entropy and hence is closely linked with the Kelvin formula. The fact that their state-of-the-art calculations pinpoint optimal doping with a maximum in the entropy represents an independent corroboration (albeit not an exact statement) that the sign-change in the thermopower (that is the OCTHH universality) does signify a QCP which has been further connected to the Mottness collapse [8, 9, 20].

Acknowledgments

AG and BSS were supported at UCSC by DOE under Grant No. FG02-06ER46319. P W P would like to acknowledge partial support from the NSF under Grant No. DMR-0940992 and the Center for Emergent Superconductivity, an Energy Frontier Research Center funded by the US Department of Energy, Office of Science, Office of Basic Energy Sciences under Award Number DE-AC0298CH1088.

References

- [1] Kadowaki K and Woods S B 1986 *Solid State Commun.* **58** 507
- [2] Tsujii N, Kontani H and Yoshimura K 2005 *Phys. Rev. Lett.* **94** 057201
- [3] Obertelli S, Cooper J R and Tallon J L 1992 *Phys. Rev. B* **46** 14928
- [4] Honma T and Hor P H 2008 *Phys. Rev. B* **77** 184520
- [5] Presland M R, Tallon J L, Buckley R G, Liu R S and Flower N E 1991 *Physica C* **176** 95
- [6] Behnia K, Jaccard D and Flouquet J 2004 *J. Phys: Condens. Matter* **16** 5187
- Sakurai J and Isikawa Y 2005 *J. Phys. Soc. Japan* **74** 1926
- Zlatić V, Monnier R, Freericks J K and Becker K W 2007 *Phys. Rev. B* **76** 085122
- [7] Leggett A J 2006 *Nat. Phys.* **2** 134
- [8] Phillips P, Choy T-P and Leigh R G 2009 *Rep. Prog. Phys.* **72** 036501
- [9] Chakraborty S, Galanakis D and Phillips P 2010 *Phys. Rev. B* **82** 214503
- [10] Peterson M R and Shastry B S 2010 *Phys. Rev. B* **82** 195105
- [11] Vidyadhiraja N S, Macridin A, Sen C, Jarrell M and Ma M 2009 *Phys. Rev. Lett.* **102** 206407
- [12] Ashcroft N and Mermin N D 1976 *Solid State Physics* (Fort Worth, TX: Harcourt Brace Jovanovich College Publishers)
- [13] Thomson W (Lord Kelvin) 1854 *Proc. R. Soc. Edinb.* **123** (Collected Papers I) 23741
- [14] Shastry B S 2009 *Rep. Prog. Phys.* **72** 016501
- [15] Loram J W, Mirza K A, Cooper J R, Liang W Y and Wade J M 1994 *J. Supercond.* **7** 243
- [16] Loram J W, Luo J, Cooper J R, Liang W Y and Tallon J L 2001 *J. Phys. Chem. Solids* **62** 59
- Loram J W, Luo J, Cooper J R, Liang W Y and Tallon J L 1994 *Physica C* **235–240** 134
- [17] Katsura S 1962 *Phys. Rev.* **127** 1508
- [18] McCoy B M, Barouch E and Abraham D B 1971 *Phys. Rev. A* **4** 2331
- [19] Nambu Y 1960 *Phys. Rev.* **117** 648
- [20] Phillips P 2011 *Phil. Trans. A* **369** 1574
- Zaanan J and Overbosch B J 2011 *Phil. Trans. A* **369** 1599
- [21] Luttinger J M 1964 *Phys. Rev. A* **135** 1505